Optimal Energy-effective Gait for Biped Robot

Lipeng Yuan[1,2]
[1]Department of Mechanical and Aerospace Engineering, College of Engineering, Cornell University
Ithaca, NY, USA
[2]School of Mechanical and Electrical Engineering, Harbin Institute of Technology, Harbin, China
e-mail: hitylp@126.com

Liming Yuan[3], Hongying Lu[4]
[3]Capital Aerospace Machinery Company, Beijing, China
[4]Department of Mechatronics and Controls, Beijing Research Institute of Precise, Beijing, China
e-mail: hitluhy@126.com

Abstract—**Although people's legs are capable of a broad range of muscle-use and gait patterns, they generally prefer just two, walking and running. A popular hypothesis regarding legged locomotion is that humans and other large animals walk and run in a manner that minimizes the metabolic energy expenditure for locomotion. Here, a mathematical model for a simple two-dimensional planar kneed walker with point feet and two bended knees is discussed. An energy-effective gait is designed by using piecewise torque method. Then, the robot model can exhibit a natural and reasonable walk on a level ground. The results can prove that the proposed optimal energy-effective gait is suitable for this kneed biped walking robot. And we also discover some walking rules maybe true through the results of optimization.**

Keywords- biped robot; optimization ; energy-effective

I. INTRODUCTION

Why do people not walk or even run with a smooth level gait[1,2], like a waiter holding two cups brim-full of boiling coffee? Why do people select walking and running from the other possibilities? We address such questions by modeling a person as a machine describable with the equations of newtonian mechanics. We hope to find how a person can move steadily with the least muscle work.

However, Walking is inherently an underactuated problem [3,4,5], which means walking systems possess less actuators than degrees of freedom. In the case of two-legged walking, it is particularly difficult to achieve both stability and efficiency. For a smaller polygon of support, bipeds need to constrain their motion considerably to achieve static stability at all times during their walking cycle. This results in high energylosses during walking and very slow and awkward movement overall. Bipeds are also not capable of walking over any sort of rough terrain, as keeping a foot flat on the ground is essential to exert the torques at the ankles.

In this paper, a mathematical model for a simple two-dimensional planar kneed walker with point feet and two bended knees is discussed. An energy-effective gait is designed by using piecewise torque method. At the same time, the tracking problem with energy-effective gait can be solved by using 'Optimized Piecewise Torque' method. As a result, the stability of the closed-loop system and the reduction of the cost are both attained. Finally, in order to demonstrate the efficiency of our design approach, the numerical result that is based on the biped robot manipulator system is given.

II. MODEL OF A KNEED BIPED

This section addresses the walking robot model. In this paper we deal with a planer biped model which has knee joints[6]. Fig. 1 shows the model of a kneed biped walking robot and Table I lists its notations and numerical settings for simulations. The robot consists of four links.

From the figure, we note that all angles are defined globally from the vertical axis. Each leg has two point masses, m_t for the upper leg (thigh) and m_s for the lower leg (shank). There is also a mass at the hip, m_H. Also, the link lengths are composed as follows: length $L = l_t + l_s$, $l_s = a_1 + b_1$ and $l_t = a_2 + b_2$.

The total walking process can be divided into four stages: 3-link phase, Active knee-lock off, Stance knee-strike, swing knee-strike, heel strike. Between them, the four time periods are t_{ks1}, t_{ks2}, t_{ks3}, t_{ks4} separately. The Fig. 2 shows the walking manner in a step cycle.

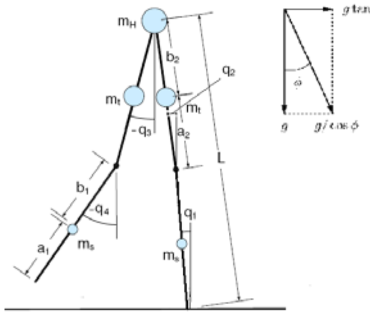

Figure 1. Four -link kneed biped model.

At the start of each step, the stance leg is modeled as a locked knee leg with an angle θ between two links, while the swing leg is modeled as two links connected by a frictionless joint. The system is governed by this dynamics until the stance legs knee is unlocked at the optimized moment. Then, the stance leg straightens out and the swing legs come forward. When the stance leg is fully extended, stance knee- strike occurs. After that the stance legs knee is locked and the swing legs straighten out, the system is governed by its unlocked swing knee dynamics until the swing leg is extended to a bended angle θ between its two links, then the swing knee-strike occurs. At the two knee-strike point, the velocities change instantly due to the collision. And immediately afterwards, we switch to a two-link system in its locked knee dynamics phase.

TABLE I. NOTATIONS AND NUMERICAL SETTINGS

Numerical Setting	Notations		
	Name	***Number***	***Unit***
m_t	Thigh mass	0.5	kg
m_s	Shank mass	0.05	kg
m_H	Hip mass	0.5	kg
a_1	Shank length (below point mass)	0.375	m
b_1	Thigh length (above point mass)	0.125	m
a_2	Shank length (below point mass)	0.175	m
b_2	Thigh length (above point mass)	0.325	m
g	Gravity acceleration	9.81	m/s^2
q_1	Stance shake leg angle		rad
q_2	Stance thigh leg angle		rad
q_3	Swing thigh leg angle		rad
q_4	Swing shake leg angle		rad
			rad
u_1	Ankle torque		N · m
u_2	Stance knee torque		N · m
u_3	Hip torque		N · m
u_4	Swing knee torque		N · m

The system remains in its locked-knee phase until the swing foot hits the ground. We model a heel-strike event here with the appropriate velocity changes. After this collision, the system returns to its initial unlocked swing knee phase.

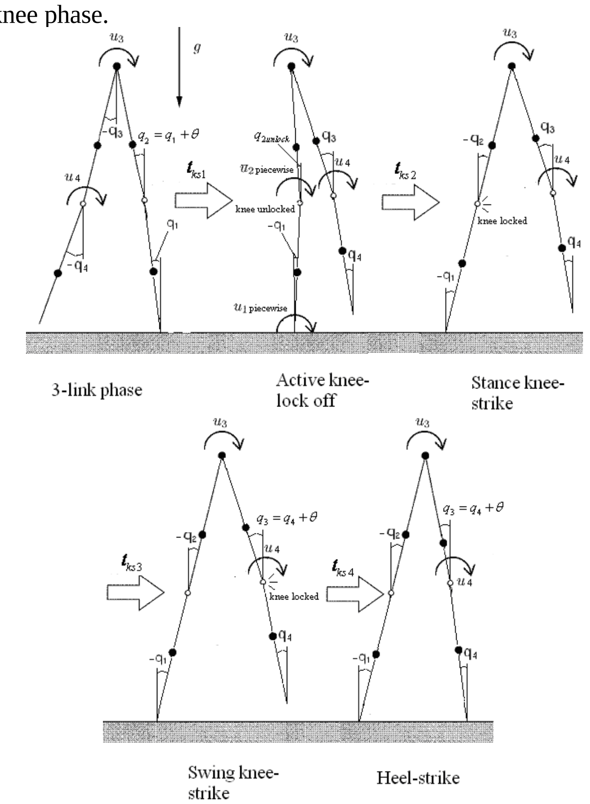

Figure 2. Walking process in a step cycle.

The robot with the suitable parameter choice is able to walk on the level ground by the effect of "virtual gravity field[7]" and additional stance knee torque toward the horizontal direction (Fig. 1).

The modeling assumptions are listed as follows.

(1) Mass: Concentrated at five points (hip, thigh and shank of stance leg and swing leg).

(2) Actuation: Full-control, i.e., a rotational actuator is assumed to be implemented at each joint as well as the contact point.

(3) Collision (heel-strike): The impact of the swing leg with the ground is assumed to be completely inelastic and without sliding.

A. Dynamic Equations

1) 3-link phase Dynamics

During the 3-link phase, the system is a three-link pendulum with bended stance leg[8]. The full equations of motion for such a system are derived using Lagrangian formulation, which is clearly described in [9]. The dynamics are shown in the standard form of planar manipulator dynamics in Equation (1). The specific inertia, velocity-dependent and gravitational matrices for the three-link pendulum are given in Equation (2).

$$H(q)\ddot{q} + B(q,\dot{q})\dot{q} + G(q) = -J^T\lambda + \tau + \tau_c \qquad (1)$$

$$H = \begin{bmatrix} H_{11} & H_{12} & H_{13} \\ H_{12} & H_{22} & H_{23} \\ H_{13} & H_{23} & H_{33} \end{bmatrix} \qquad (2a)$$

$$B = \begin{bmatrix} 0 & h_{12}\dot{q}_3 & h_{13}\dot{q}_4 \\ h_{21}\dot{q}_1 & 0 & h_{23}\dot{q}_4 \\ h_{31}\dot{q}_1 & h_{32}\dot{q}_3 & 0 \end{bmatrix} \qquad (2b)$$

$$G = \begin{bmatrix} \begin{pmatrix} \left(m_s \cdot l_t + m_t\left(l_t + a_2\right) + m_t \cdot a_2\right)\cdot \sin\left(\phi - q_1 - \theta\right) \\ +\left(m_s \cdot a_1 + \left(m_h + m_s + 2\cdot m_t\right)\cdot l_s\right)\cdot \sin\left(\phi - q_1\right) \end{pmatrix} g \\ -\left(m_t b_2 + m_s l_t\right) g \sin\left(\phi - q_3\right) \\ -m_s b_1 g \sin\left(\phi - q_4\right) \end{bmatrix} \qquad (2c)$$

And $J^T\lambda$ is the constraint force at knee-joint. τ is the control input and τ_c is the vector due to the environmental forces of the robot.

Given appropriate mass distributions and initial conditions, the swing leg bends the knee as it swings forward. At the optimized instant the stance leg knee is unlocked, the stance leg straightens out and at the same time, the swing leg comes forward.

2) Active knee-lock off Dynamics

After the optimized stance leg knee unlocked moment, an additional control torque should be added on knee of the stance leg. The system is a four-link pendulum and the dynamics for the new unlocked system are shown in Equation (3) for completeness.

At the instant the stance upper leg straightens out and aligns with the lower leg, a stance leg knee strike collision is modeled.

$$H=\begin{bmatrix} H_{11} & H_{12} & H_{13} & H_{14} \\ H_{12} & H_{22} & H_{23} & H_{24} \\ H_{13} & H_{23} & H_{33} & H_{34} \\ H_{14} & H_{24} & H_{34} & H_{44} \end{bmatrix} \tag{3a}$$

$$B=\begin{bmatrix} 0 & h_{12}\dot{q}_2 & h_{13}\dot{q}_3 & h_{14}\dot{q}_4 \\ h_{21}\dot{q}_1 & 0 & h_{23}\dot{q}_3 & h_{24}\dot{q}_4 \\ h_{31}\dot{q}_1 & h_{32}\dot{q}_2 & 0 & h_{34}\dot{q}_4 \\ h_{41}\dot{q}_1 & h_{42}\dot{q}_2 & h_{43}\dot{q}_3 & 0 \end{bmatrix} \tag{3b}$$

$$G=\begin{bmatrix} \left(\left(m_h+m_s+2m_t\right)l_s+m_s a_1\right) g\sin\left(\phi-q_1\right) \\ \left(\left(m_h+m_s+2m_t\right)l_t+m_t a_2\right) g\sin\left(\phi-q_2\right) \\ -\left(m_t b_2+m_s l_t\right) g\sin\left(\phi-q_3\right) \\ -m_s\cdot b_1\cdot g\sin\left(\phi-q_4\right) \end{bmatrix} \tag{3c}$$

3) Stance Knee-Lock Dynamics

After the stance leg knee-strike, the swing lower leg straightens out until it is extended to a bended angle θ with the upper leg. During this swing phase, the system is a three-link pendulum. The dynamics are shown in Equation (4) for completeness.

$$H=\begin{bmatrix} H_{11} & H_{12} & H_{13} \\ H_{12} & H_{22} & H_{23} \\ H_{13} & H_{23} & H_{33} \end{bmatrix} \tag{4a}$$

$$B=\begin{bmatrix} 0 & h_{12}\dot{q}_3 & h_{13}\dot{q}_4 \\ h_{21}\dot{q}_1 & 0 & h_{23}\dot{q}_4 \\ h_{31}\dot{q}_1 & h_{32}\dot{q}_3 & 0 \end{bmatrix} \tag{4b}$$

$$G=\begin{bmatrix} \left(m_s a_1+m_t\left(l_s+a_2\right)+\left(m_h+m_s+m_t\right)L\right) g\sin\left(\phi-q_1\right) \\ -\left(m_t b_2+m_s l_t\right) g\sin\left(\phi-q_3\right) \\ -m_s b_1 g\sin\left(\phi-q_4\right) \end{bmatrix} \tag{4c}$$

At the instant the lower leg straightens out and extends to a bended angle θ with the upper leg, a swing leg knee-strike collision is modeled.

4) 2-link phase Dynamics

After the swing leg knee-strike, the two knees remain locked and we switch to double-link pendulum dynamics. The remainder of the swing phase occurs with one straight leg and one bended leg. The dynamics for the new-locked system are exactly those of the compass gait dynamics but with a different mass configuration. They are shown in Equation (5) for completeness.

When the swing foot touches the ground, we model another discrete event, the heel-strike collision. After this, we switch the stance and swing legs. This completes a full step, and we begin a new step using the three-link with bended stance leg unlocked dynamics.

$$H=\begin{bmatrix} H_{11} & H_{12} \\ H_{12} & H_{22} \end{bmatrix} \tag{5a}$$

$$B=\begin{bmatrix} 0 & h\dot{q}_3 \\ -h\dot{q}_1 & 0 \end{bmatrix} \tag{5b}$$

$$G=\begin{bmatrix} \left(m_s a_1+m_t\left(l_s+a_2\right)+\left(m_h+m_s+m_t\right)L\right) g\sin\left(\phi-q_1\right) \\ -\left(\left(m_t b_2+m_s l_t\right)\sin\left(\phi-q_3\right)+m_s b_1\sin\left(\phi+\theta-q_3\right)\right) g \end{bmatrix} \tag{5c}$$

5) Stance knee-strike Dynamics

We model the stance leg knee strike as a discrete collision event in a four-link chain and switch to three-link chain model afterwards. Since the only external force on this system is at the stance foot, angular momentum is preserved for the entire system about the stance foot and for the swing leg about the hip and for the lower link of swing leg about its knee. Looking at the upper link of stance leg, however, the Stance knee-strike acts as an external impulse. Therefore, angular momentum is not conserved about the stance leg knee.

Using these conservation equations, we obtain the post-collision velocities for the fist and the last two joint angles. The second joint angle corresponding to the knee is locked after the collision. Therefore, its post-collision velocity will be that of the first link. We express the change in velocities as:

$$Q^{+}\begin{bmatrix} \dot{q}_1^{+} \\ \dot{q}_3^{+} \\ \dot{q}_4^{+} \end{bmatrix}=Q^{-}\begin{bmatrix} \dot{q}_1^{-} \\ \dot{q}_2^{-} \\ \dot{q}_3^{-} \\ \dot{q}_4^{-} \end{bmatrix} \tag{6}$$

$$\dot{q}_1^{+}=\dot{q}_2^{+}$$

6) Swing Knee-strike Dynamics

We model the swing knee-strike as a discrete collision event in a three-link chain and switch to the compass gait model afterwards. Since the only external force on this system is also at the stance foot, angular momentum is preserved for the entire system about the stance foot and for the swing leg about the hip.

Using these conservation equations, we obtain the post-collision velocities for the first two joint angles of the three-link chain. The third joint angle corresponding to the swing knee is locked after the collision. Therefore, its post-collision velocity will be that of the second link. We express the change in velocities as:

$$Q^{+}\begin{bmatrix} \dot{q}_1^{+} \\ \dot{q}_3^{+} \end{bmatrix}=Q^{-}\begin{bmatrix} \dot{q}_1^{-} \\ \dot{q}_3^{-} \\ \dot{q}_4^{-} \end{bmatrix} \tag{7}$$

$$\dot{q}_2^{+}=\dot{q}_1^{+} \qquad \dot{q}_3^{+}=\dot{q}_4^{+}$$

7) Heel-strike Dynamics

The heel-strike is modeled as an inelastic collision about the colliding foot. This heel-strike event is, again, identical to the heel strike for the compass gait. Since the only external force occurs at the point of impact, there are no moments created around this point and therefore, no external torques act on the system. Angular momentum is then conserved for the entire system about the colliding foot and for the swing leg after impact about the hip.

Right after the event, the model switches both legs and the impact foot becomes the new stance foot. The model also switches back to the bended stance leg three-link dynamics to start a new step cycle. The third joint angle starts with θ angular difference position and the same velocity as the second one. This collision event is expressed in Equation (8).

$$\begin{bmatrix} q_1^+ \\ q_2^+ \\ q_3^+ \\ q_4^+ \end{bmatrix} = \begin{bmatrix} 0 & 1 & -1 \\ 0 & 1 & 0 \\ 1 & 0 & 0 \\ 1 & 0 & 0 \end{bmatrix} \cdot \begin{bmatrix} q_1^- \\ q_3^- \\ \theta \end{bmatrix} \tag{8}$$

$$Q^+ \begin{bmatrix} \dot{q}_1^+ \\ \dot{q}_3^+ \end{bmatrix} = Q^- \begin{bmatrix} \dot{q}_1^- \\ \dot{q}_3^- \end{bmatrix}$$

$$\dot{q}_2^+ = \dot{q}_1^+ \qquad \dot{q}_3^+ = \dot{q}_4^+$$

B. The Optimized Numerical Simulations Result

By using the 'SNOPT' software and according to the optimizing target and constraint condition, we can get the result which makes the total actuator's torque energy minimal.

A limit cycle for the upper link of one leg is shown in Figure 3.

The instantaneous velocity changes from the stance kneestrike, swing kneestrike and heelstrike events can be observed in this limit cycle as straight lines where the cycle jumps with the instantaneous velocity changes while the positions remain the same.

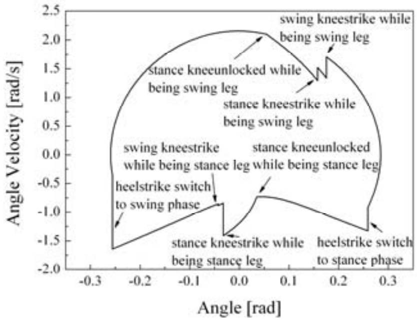

Figure 3. Limit cycle trajectory for the upper link of one leg

On the other hand, the kneeunlocked event will happen just before the upper link of the stance leg become perpendicular to the level ground, the optimized $q_{2unlock}$ is approximately 2.06°. the kneeunlocked event and the additional piecewise torque $u_{2\,piecewise}$ produce a push off effect on the knee, and following this, the stance kneestrike event will happen just after the upper link swing angle q_2 pass across the 0°.

We see that the limit cycle closely resembles that of the compass gait. There is a swing phase (top half of the curve) and a stance phase (bottom half of curve) for each leg. In contrast with the compass gait, however, in addition to the two heel-strikes, there are four more instantaneous velocity changes produced by the stance kneestrikes and swing kneestrikes and a knee push off by piecewise torque $u_{2\,piecewise}$. This limit cycle is traversed clockwise.

And Fig. 6 shows the actuator's torques of the four joint torques of the piecewise control in one step.

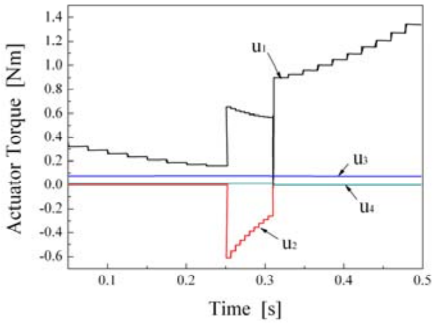

Figure 4. The actuator's torques of the system with piecewise control

In these figures the walking gait is an inverted pendulum with heel-strike and push-off stages, and we can see that if we use the piecewise function on the ankle's torque u_1, and the period piecewise function on the stance knee torque u_2 to drive, there are not only the heel-strike torque, but also the ankle push-off torque and knee push-off torque. And in this case, the knee push-off torque is very helpful for reducing the consuming power during biped walking. On the other hand, the hip's torque u_3 and the swing knee's torque u_4 are both constant, this is very important feature for the stability of biped robot's posture.

Indeed, real human ankle joint should have heel-strike and push-off toques at the beginning and ending of one step [10]. The stance knee has a push-off toque before the upper link of the stance leg become perpendicular to the level ground. And the hip joint does approximately perform a positive constant-like torque during one step. The swing knee joint torque of the swing leg should also be approximately constant before the knee is locked.

III. CONCLUSIONS AND FUTURE WORK

A popular hypothesis regarding legged locomotion is that humans and other large animals walk and run in a manner that minimizes the metabolic energy expenditure for locomotion.

And in this thesis, a hybrid model for a passive 2D walker with knees and point feet is presented. An energy-effective gait is designed by using piecewise torque method. The stability of the closed-loop system and the reduction of the cost are both attained. At low speeds, the optimization discovers a natural and reasonable walk on a level ground. The results can prove that the proposed optimal gait is effective and stable for this kneed biped walking robot.

REFERENCES

[1] A. D. Kuo, J. M. Donelan, and A. Ruina. Energetic consequences of walking like an inverted pendulum: step-to-step transitions. Exer.

Sport Sci. Rev., 33:88–97, 2005.

[2] N. Rashevsky. Studies in the physicomathematical theory of organic form. Bull. Math. Biophysics., 6:1–59, 1944.

[3] R. McN. Alexander. Elastic mechanisms in animal movement. Cambridge University Press, Cambridge., 1988.

[4] T.A. McMahon and G.C. Cheng. The mechanics of running: how does stiffness couple with speed? J. Biomech., 23, Suppl.1:65–78, 1990.

[5] R. McN. Alexander. Mechanics of bipedal locomotion., volume 1, page 493504. Pergamon Press, New York, 1976.

[6] Vanessa F. Hsu Chen. Passive Dynamic Walking with Knees: A Point Foot Model. Massachusetts Institute of Technology Press, Massachusetts., 2007.

[7] F. Asano, M. Yamakita and K. Furuta. “Stabilizing control of passive biped robot and its application to active walking,” in Proc. 5th Int. Conf. Artif. Life and Robot., vol. 2, pp. 503–506, 2000.

[8] K Kaneko, F. Kanehiro, S. Kajita, H. Hirukawa, T. Kawasaki, , M. Hirata, K.Akachi, and T. Isozumi. Humanoid robot hrp-2. In Proc. of the IEEE Conf. on Robotics and Automation, pages 1083–1090, 2004.

[9] Jean-Jacques E. Slotine and Weiping Li. Applied Nonlinear Control. Prentice Hall, October 1990.

[10] Manoj Srinivasan and Andy Ruina. Computer optimization of a minimal biped model discovers walking and running. Nature Vol 439: 72-75, 2006.